AT&T Bell Laboratories Technical Journal
Vol. 63, No. 9, November 1984
Printed in U.S.A.

Spatial Filtering Radio Astronomical Data: One-Dimensional Case

By H. E. ROWE*

(Manuscript received May 26, 1983)

Radio astronomical measurements of radio brightness are made by pointing an antenna at a regular array of points in the sky and measuring the received noise power at each point. In the absence of receiver noise, the measured brightness is the convolution of the true brightness distribution with the antenna effective area (i.e., receiving power pattern), evaluated at the point of observation. Front-end noise in the radiometer receiver adds fluctuations inversely proportional to the observing time at each measured point. From such data, we calculate optimum mean-square estimates for two quantities: measured brightness between observations, and true brightness at and between observations. The first is interpolation; the second, called restoration, partially deconvolves the antenna pattern from the measured data. We determine the errors associated with each, as functions of: (1) receiving antenna pattern, (2) separation between observations, and (3) radiometer output signal-to-noise ratio. These results permit the construction of maps of measured and true brightness, with known mean-square errors. In this paper we study the one-dimensional version of this problem, assuming a large number of measured points. We find that measured points should be separated by about half the (full) 3-dB beamwidth for conventional antennas. Restoration is more costly than interpolation.

I. INTRODUCTION

Radio astronomical measurements of radio brightness are made by pointing an antenna at a regular array of points in the sky and

* AT&T Bell Laboratories.

measuring the power of the random signal at the antenna output with a radiometer receiver. The measured points may lie in a square array; alternatively, we may wish to consider a hexagonal array, or irregular arrays of measured points.

We denote the antenna output power for each measured point as the measured brightness; the measured brightness is the convolution of the true brightness distribution with the antenna receiving power pattern, evaluated for the particular point under study. The radiometer receiver has a "signal" output proportional to the measured brightness, plus a "noise" output, due principally to the receiver front-end noise (which far exceeds the received power at the antenna output). The receiver "noise" output has mean-square value proportional to the receiver noise temperature squared and inversely proportional to the observation (or integration) time (see the Appendix of Ref. 1).

We wish to construct maps of radio brightness from such discrete measurements. First, let us estimate the measured brightness between observations, i.e., what we would have observed if we had pointed the antenna in between the actual measured points. This has been called "interpolation".[2]

However, the antenna does not have an infinitely narrow beam, and hence the measured brightness is a smoothed version of the true brightness. We wish to deconvolve the antenna pattern so as to determine the true brightness distribution as closely as possible. This has been called "restoration".[2]

For a given antenna, two factors that limit accuracy for either interpolation or restoration are the separation between measurements and receiver noise.

Suppose first that receiver noise is absent. Measurements that are too widely separated will provide little information about the brightness at points far from the observations. However, measurements that are too close yield redundant information. Receiver noise limits the accuracy for both interpolation and restoration; however, restoration is much more severely affected since it involves deconvolution of the antenna pattern.

Receiver noise at each point is inversely proportional to the observation time at that point, as noted above. Therefore, if we allot a given total amount of time for a particular region of the sky, we can trade off separation between observations against signal-to-noise ratio. That is, we may choose few widely spaced observations, with long observing times and hence small noise, or alternatively many closely spaced observations with short observing times and hence large noise.

We require the optimum mean-square estimates for interpolation and restoration. These results will yield the best angular separation between observations, as well as the relative costs of restoration and

interpolation. The optimum estimates depend on the statistical model assumed for the brightness distribution; we assume the brightness varies rapidly compared to the antenna beamwidth.

This paper explores the one-dimensional version of this problem, an antenna with a strip aperture and a fan beam. We assume an infinite number of equally spaced observed points. The mean-square interpolation and restoration errors are determined as functions of the separation between observations, antenna width, and signal-to-noise ratio for two (one-dimensional) antenna illumination functions:

1. Uniform illumination (maximum gain antenna)
2. Truncated Gaussian illumination with a 15-db taper.

For this one-dimensional problem we find that observations should be separated by about half the (full) 3-db beamwidth in the case of truncated Gaussian illumination, which corresponds to a normal antenna. For a given error, restoration is much more expensive than interpolation in observing time.

The present results serve as a guide for similar studies of the real two-dimensional case, i.e., an antenna with a circular aperture and a pencil beam.

II. SAMPLED-DATA MODEL FOR MEASUREMENT OF A ONE-DIMENSIONAL INCOHERENT FIELD BY A FAN-BEAM ANTENNA

Consider a strip antenna with its aperture located in the x-y plane, as we see in Fig. 1. The aperture has width W along the x axis, and is centered about the y-z plane; the aperture extends to $\pm\infty$ along the y axis. All field quantities are assumed to be independent of y; therefore, the antenna has a fan beam, with gain and effective width (as transmitting and receiving antenna, respectively) that depend on only the angular coordinate t, measured in the x-z plane, of a cylindrical coordinate system shown in Fig. 1. The angle t is not measured in radians, but rather is suitably normalized to simplify the following relations; the details of this normalization are unnecessary for our present purposes. Suppose for the present that the antenna beam points along the z axis; denote the effective width by $A(t)$, with Fourier transform $\mathscr{A}(f)$.

Let the aperture electric field (in the x-y plane) be polarized along the x direction, and denoted by $E(x)$. Then for narrow-beam antennas $\mathscr{A}(f) \propto E(f) \circledast E^*(-f)$, where we use the symbol $\circledast$ to denote convolution throughout. Since $E(x)$ is zero outside of the aperture, i.e., for $|x| > W/2$, it follows that $\mathscr{A}(f)$, the Fourier transform of the effective width $A(t)$, is strictly bandlimited to $|f| < W$.

We measure a one-dimensional, incoherent field, with radio brightness $x(t)$, by pointing this antenna in direction t, denoting the power out of the antenna feed as $x_o(t)$, which we call the measured brightness.

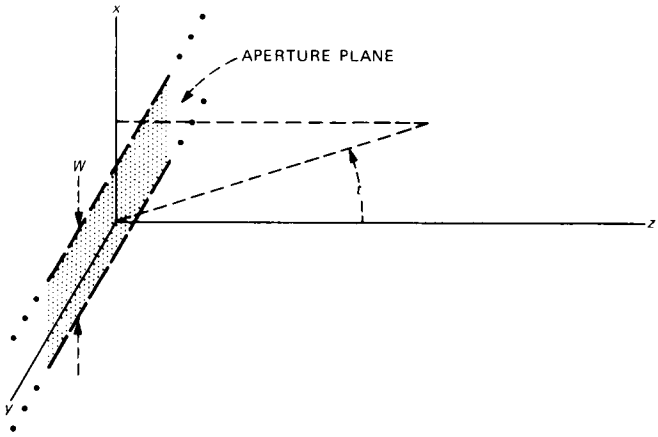

Fig. 1—Geometry of strip antenna.

The convolution of $x(t)$ with $A(t)$ is $x_o(t) = x(t) \circledast A(t)$. Such measurements are repeated at equally spaced angles $t = kT, \cdots, -1, 0, 1, \cdots$, providing measured brightness samples $x_o(kT)$. Independent noise is added by the receiver to these samples; and from these noisy samples we wish the optimum linear estimate of the brightness $x(t)$ (restoration), or of the measured brightness $x_o(t)$ (interpolation). Figure 2a shows these measurements.

The symbols in Fig. 2 have the following definitions for the one-dimensional antenna problem:

t	normalized angular coordinate.
f	normalized spatial frequency.
$x(t)$	radio brightness (one-dimensional).
W	antenna width.
$E(x)$	aperture electric field; zero for $\|x\| > W/2$.
$A(t)$	effective width (as a receiving antenna).
$\mathscr{A}(f)$	Fourier transform of $A(t)$; approximately proportional to $E(f) \circledast E^*(-f)$ in narrow-beam approximation, strictly bandlimited to $\|f\| < W$.
kT	observing angles.
$x_o(kT)$	receiver signal samples.
$n(t)$	random function; $n(kT)$ = receiver noise samples, independent for different k.
N	$= \langle n^2(kT) \rangle$, expected sample noise power; proportional to receiver noise temperature squared and inversely proportional to integration time.
$h(t)$	weight function for data samples $x_o(kT) + n(kT)$.
$H(f)$	Fourier transform of $h(t)$; transfer function used as spatial filter on data samples.

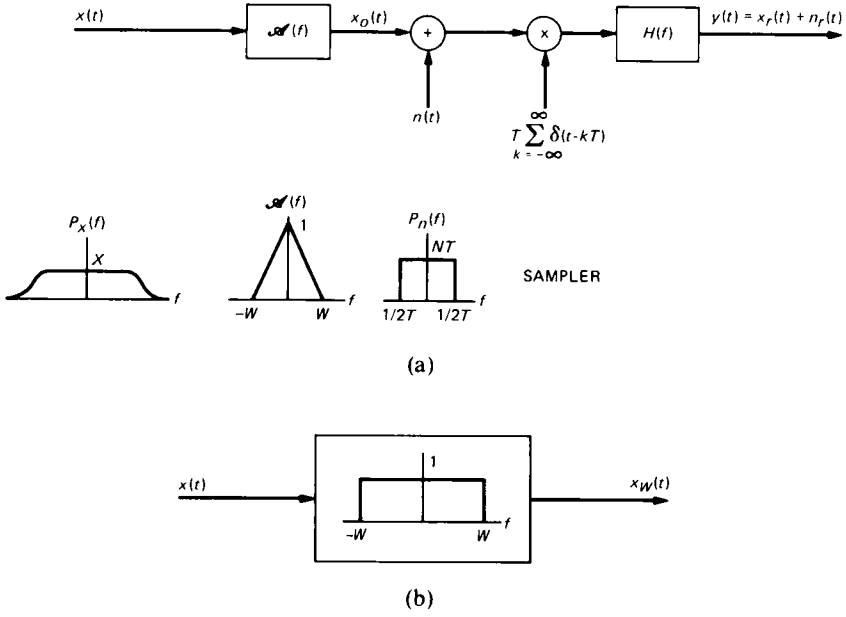

Fig. 2—Sampling and reconstruction of a stationary random function. (a) Wideband input—general input and reconstruction filters. (b) Bandlimited version of input.

The effective width $A(t)$ and its Fourier transform $\mathscr{A}(f)$ satisfy the following relations in the narrow-beam approximation, with suitable normalization of the angular coordinate t:

$$0 \leq A(t) \leq W$$

$$\mathscr{A}(f) = \frac{E(f) \circledast E^*(-f)}{\int_{-\frac{W}{2}}^{\frac{W}{2}} |E(x)|^2 dx} = \frac{\int_{\max\left(-\frac{W}{2}, -\frac{W}{2}+f\right)}^{\min\left(\frac{W}{2}, \frac{W}{2}+f\right)} E(x)E^*(x-f)dx}{\int_{-\frac{W}{2}}^{\frac{W}{2}} |E(x)|^2 dx}$$

$$\mathscr{A}(0) = \int_{-\infty}^{\infty} A(t)dt = 1; \qquad \mathscr{A}(f) = 0, \ |f| > W. \tag{1}$$

We do not consider super-gain antennas in the narrow-beam approximation. Maximum effective width, $A(0) = W$, is attained for uniform illumination of the antenna aperture with zero phase error, $E(x) = 1$ for $|x| < W/2$, i.e., for an antenna with maximum on-axis gain. For this case $\mathscr{A}(f)$ is the triangular function illustrated in Fig. 2a:

$$\mathscr{A}(f) = \begin{cases} 1 - |f/W|, & |f| \le W \\ 0, & |f| \ge W. \end{cases} \tag{2}$$

Alternatively, the block diagram of Fig. 2a may be considered to represent a sampled-data system. An input time function $x(t)$ is convolved with $A(t)$ or equivalently filtered by its Fourier transform $\mathscr{A}(f)$, producing $x_o(t)$. Noise $n(t)$ is added to $x_o(t)$, and their sum is sampled to produce noisy samples $x_o(kT) + n(kT)$, with different noise samples independent. The noisy samples are filtered by $H(f)$ to produce optimum linear estimates of $x(t)$ or of $x_o(t)$. Much of the following discussion will be carried out for this sampled-data system, which is equivalent to the measurement of a one-dimensional incoherent field by a one-dimensional antenna.

It remains to specify the spectra of the input signal $x(t)$ and the noise $n(t)$ in Fig. 2a. We have assumed the radio brightness $x(t)$ varies rapidly with respect to the antenna beamwidth, i.e., with respect to the width of $A(t)$; this would arise, for example, from a random distribution of point sources, dense compared to the antenna beamwidth. Since power is positive, brightness is also positive, and consequently, $\langle x(t) \rangle \ge 0$. We assume that the dc component of $x(t)$ is deterministic (see Appendix A), and we treat it separately. The ac component of $x(t)$ has power spectrum $P_x(f)$ essentially white, i.e., wide compared to the bandwidth W of $\mathscr{A}(f)$; we denote the spectral density of $P_x(f)$ within this band $|f| < W$ by X.

Finally, the noise spectrum $P_n(f)$ of Fig. 2a—white, bandlimited, with spectral density NT in the band $|f| < 0.5/T$—will yield independent noise samples $n(kT)$ with power N, as we assumed above.

Consider the block diagram of Fig. 2a as a sampled-data system. The stationary input $x(t)$ is filtered by $\mathscr{A}(f)$, which is bandlimited to W as indicated, producing the quantity $x_o(t)$. Since $P_x(f)$, the power spectrum of $x(t)$, is white with spectral density X within this band, $x_o(t)$ at the output of $\mathscr{A}(f)$ will have power spectrum

$$P_{x_o}(f) = |\mathscr{A}(f)|^2 P_x(f) \approx X \cdot |\mathscr{A}(f)|^2. \tag{3}$$

Noise is added, and the noisy filtered output is sampled at interval T; the noise samples are independent, with power N. Finally, a reconstruction filter $H(f)$ yields an output signal $x_r(t)$ and noise $n_r(t)$.

All frequency components of the original input $x(t)$ outside the band W, $|f| > W$ have been lost. Therefore, we can only estimate the bandlimited version of $x(t)$ (Fig. 2b), i.e.:

$$x_W(t) = x(t) \circledast 2W \frac{\sin 2\pi W t}{2\pi W_t}. \tag{4}$$

Alternatively, we might wish to estimate $x_o(t)$, at the output of the

filter $\mathscr{A}(f)$ of Fig. 2a. Consequently, we define the following two errors:

$$e_W(t) \equiv x_r(t) - x_W(t).$$
$$e_o(t) \equiv x_r(t) - x_o(t). \tag{5}$$

The quantities $e(t)$, which represent the errors in the absence of noise, consist of linear distortion plus aliasing. Noting that $x(t)$ and $n(t)$, and hence $x_r(t)$ and $n_r(t)$, are independent, the output error $e(t)$ is independent of the output noise $n_r(t)$. Consequently, the total mean-square deviation between desired and actual output is given in each of the two cases as follows:

$$\overline{\langle d_W^2(t)\rangle} \equiv \overline{\langle [y(t) - x_W(t)]^2\rangle} = \overline{\langle e_W^2(t)\rangle} + \overline{\langle n_r^2(t)\rangle}.$$
$$\overline{\langle d_o^2(t)\rangle} \equiv \overline{\langle [y(t) - x_o(t)]^2\rangle} = \overline{\langle e_o^2(t)\rangle} + \overline{\langle n_r^2(t)\rangle}. \tag{6}$$

Here the symbols $\langle\ \rangle$ indicate an ensemble average and the symbol $\overline{}$ indicates a time average over one sampling interval T, in the sampled-data model of Fig. 2. The quantities in (6) will depend on $H(f)$, the transfer function of the reconstruction filter. We might want to minimize either of them; the transfer functions that do so are denoted $H_W(f)$ and $H_o(f)$, respectively. By analogy to the terminology used for the two-dimensional antenna problem in Section I,[2] we call the estimation of $x_o(t)$ "interpolation", and the estimation of $x_W(t)$ "restoration" in the present one-dimensional problem.

We distinguish two cases:

$$WT < 0.5; \quad \text{oversampled}$$
$$WT > 0.5; \quad \text{undersampled}.$$

In the undersampled case the $\overline{\langle e^2(t)\rangle}$ of (6) comprise both linear distortion and aliasing; in the oversampled case aliasing is absent. The $\overline{\langle n_r^2(t)\rangle}$ of (6) arise from noise in both cases.

The oversampled case is the simplest. Here aliasing is absent, as we noted above. Both the linear distortion and, as we see below, the output noise are stationary. Consequently, we may drop the time-averaging symbols throughout (6).

In the undersampled case both the aliasing and the output noise are nonstationary. While the time-averaged quantities in (6) are easy to compute, we need in addition these quantities as functions of time, i.e., with the time-averaging symbols in (6) removed.

The optimum filters $H_W(f)$ and $H_o(f)$, which minimize the mean-square deviations in (6), are Wiener least-square-error filters. We show for the undersampled case that Wiener filters minimize not only the time-averaged mean-square deviations, but also the time-depend-

ent mean-square deviations. The spectra of linear distortion, aliasing, and noise are all simply additive.

Such filters operate on all the data samples $x_o(kT) + n(kT)$, $-\infty < k < \infty$. In practice we will estimate $x_W(t)$ or $x_o(t)$ from a finite number of data samples. Here it is no longer possible to separate the contributions of linear distortion and aliasing; the errors are nonstationary in both the undersampled and oversampled cases. We defer treatment of this problem to a future paper.

We treat these various cases below as an introduction to the two-dimensional antenna case. We take the following quantities as given:

X	$\lim_{f \to 0} P_x(f)$, $f \neq 0$, low-frequency limit of continuous component of spectral density of $x(t)$.
$\langle x(t) \rangle$	expected value of $x(t)$.
T	sampling interval.
N	mean-square sample noise, independent for different samples.
$\mathscr{A}(f)$	input filter transfer function: $\mathscr{A}(0) = 1$; $\mathscr{A}(f) = 0$, $\lvert f \rvert \geq W$.

We assume

$$\lim_{\epsilon \to 0} \int_{-\epsilon}^{\epsilon} P_x(f) df = \langle x(t) \rangle^2. \tag{7}$$

III. GENERAL FILTERS

The signal and noise outputs in Fig. 2a are given in terms of the measured sample values as follows:

$$x_r(t) = T \sum_{k=-\infty}^{\infty} x_o(kT) h(t - kT)$$

$$n_r(t) = T \sum_{k=-\infty}^{\infty} n(kT) h(t - kT). \tag{8}$$

The weight function, $h(t)$, is the impulse response of the reconstruction filter of Fig. 2, i.e., the Fourier transform of $H(f)$. The output $y(t)$ may be intended as an estimate either of $x_W(t)$ or of $x_o(t)$ of Fig. 2, with errors $e_W(t)$ or $e_o(t)$, respectively, (5), and noise $n_r(t)$.

The power spectra of these errors are given, respectively, as follows:

$$P_{e_W}(f) = \lvert H(f) \rvert^2 \sum_{\substack{n=-\infty \\ n \neq 0}}^{\infty} P_{x_o}\left(f - \frac{n}{T}\right) + \lvert 1 - H(f)\mathscr{A}(f) \rvert^2 P_{x_W}(f)$$

$$P_{e_o}(f) = \lvert H(f) \rvert^2 \sum_{\substack{n=-\infty \\ n \neq 0}}^{\infty} P_{x_o}\left(f - \frac{n}{T}\right) + \lvert 1 - H(f) \rvert^2 P_{x_o}(f). \tag{9}$$

Here $P_{x_o}(f)$ and $P_{x_W}(f)$ are related by (3) and (4):

$$P_{x_o}(f) = |\mathscr{A}(f)|^2 \cdot P_{x_W}(f); \qquad P_{x_W}(f) = \begin{matrix} X, & |f| < W \\ 0, & |f| \geq W. \end{matrix} \tag{10}$$

The first terms of (9) represent aliasing; the second terms represent linear distortion of the signal. The mean-square errors are[3,4]

$$\overline{\langle e^2(t)\rangle} = \langle \overline{e^2(t)}\rangle = \int_{-\infty}^{\infty} P_e(f)df, \tag{11}$$

where $e(t)$ represents either $e_W(t)$ or $e_o(t)$. The time average, indicated by $\overline{}$ in (11), may be taken over any integral number of sampling intervals T, in view of the stationarity of $x(t)$.

The output noise power spectrum is

$$P_{n_r}(f) = NT \cdot |H(f)|^2. \tag{12}$$

The mean-square output noise is

$$\overline{\langle n_r^2(t)\rangle} = \langle \overline{n_r^2(t)}\rangle = NT \int_{-\infty}^{\infty} |H(f)|^2 df, \tag{13}$$

where again the time average $\overline{}$ may be taken over any integral number of sampling intervals T.

$\mathscr{A}(f)$ is strictly bandlimited to $|f| < W$; then from (3) or (10)

$$P_{x_o}(f) = 0, \qquad |f| \geq W. \tag{14}$$

The output $y(t)$ contains only alias and noise components outside the band $|f| \geq W$; the reconstruction filter transfer function should certainly be zero there. Consequently, we assume

$$H(f) = 0, \qquad |f| \geq W \tag{15}$$

throughout the remainder of this paper.

By (14) if the sampling is fast enough, $WT < 0.5$, alias and signal components are separated in (9). Since $H(f)$ satisfies (15), aliasing is absent in the output; both $x_r(t)$ and $n_r(t)$ are stationary, and we may drop the time averages $\overline{}$ in (11) and (13). Thus in the oversampled case:

$$\left.\begin{aligned} \langle e_W^2(t)\rangle &= \int_{-W}^{W} |1 - H(f)\mathscr{A}(f)|^2 P_x(f)df \\ \langle e_o^2(t) &= \int_{-W}^{W} |1 - H(f)|^2 P_{x_o}(f)df \\ \langle n_r^2(t)\rangle &= NT \int_{-W}^{W} |H(f)|^2 df \end{aligned}\right\} W < \frac{1}{2T}. \tag{16}$$

In the undersampled case the expected values on the left-hand side of (16) become periodic functions of time. We make the additional ad hoc assumption that

$$W < \frac{1}{T}; \tag{17}$$

then from (14) no more than two terms overlap in (9). This assumption is appropriate for the antenna problem described in Sections I and II. Then from Appendix B:

$$\langle e_W^2(t)\rangle = 2\int_0^W \left| e^{-j2\pi\frac{t}{T}} H\left(f - \frac{1}{T}\right)\mathscr{A}(f) - 1 + H(f)\mathscr{A}(f)\right|^2 \cdot P_{x_W}(f)df$$

$$\langle e_o^2(t)\rangle = 2\int_0^W \left| e^{-j2\pi\frac{t}{T}} H\left(f - \frac{1}{T}\right) - 1 + H(f)\right|^2 P_{x_o}(f)df$$

$$\langle n_r^2(t)\rangle = 2NT\int_0^{\frac{1}{2T}} \left| e^{-j2\pi\frac{t}{T}} H\left(f - \frac{1}{T}\right) + H(f)\right|^2 df. \tag{18}$$

Time averaging (18) subject to (15) yields directly the results obtained from (9) and (11) and from (13). This is readily seen by substituting

$$\overline{|e^{-j2\pi\frac{t}{T}}P + Q|^2} = |P|^2 + |Q|^2 \tag{19}$$

into (18), with appropriate choices for P and Q. Finally, the results (18) simplify when $H(f)$ and $\mathscr{A}(f)$ are real. This special case is significant because, as we show in Section IV, the optimum filter $H_o(f)$ is always real, and the optimum filter $H_W(f)$ is real for real $\mathscr{A}(f)$, i.e., for antenna illumination with zero phase error. These simplifications are obtained by substituting

$$|e^{-j2\pi\frac{t}{T}}P + Q|^2 = P^2 + Q^2 + 2PQ\cos 2\pi\frac{t}{T}, \quad P \text{ and } Q \text{ real}, \tag{20}$$

into (18).

IV. OPTIMUM FILTERS

The results of optimum linear mean-square filter theory are summarized as follows. Figure 3 shows an input signal $x_i(t)$ filtered by an input filter with transfer function $\mathscr{A}(f)$, to yield a measured signal $x_o(t)$. Noise $\nu(t)$ is added to $x_o(t)$. We obtain linear least-mean-square

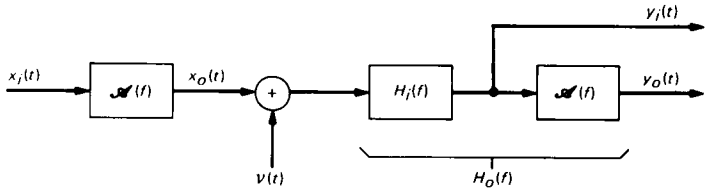

Fig. 3—Optimum linear mean-square estimation.

estimates for the input signal $x_i(t)$ and the measured signal $x_o(t)$ by filtering $x_o(t) + \nu(t)$ by $H_i(f)$ and $H_o(f)$, respectively, as shown in Fig. 3. The transfer functions of these Wiener filters are given as follows:[5]

$$H_i(f) = \frac{1}{\mathscr{A}(f) + \dfrac{P_\nu(f)}{\mathscr{A}^*(f)P_{x_i}(f)}} \tag{21}$$

$$H_o(f) = \frac{P_{x_o}(f)}{P_{x_o}(f) + P_\nu(f)} = \mathscr{A}(f)H_i(f). \tag{22}$$

Here $P_{x_i}(f)$, $P_{x_o}(f)$, and $P_\nu(f)$ are the power spectra of the input signal $x_i(t)$, the measured signal $x_o(t)$ at the output of the filter $\mathscr{A}(f)$, and of the additive noise $\nu(t)$, respectively. Note that

$$P_{x_o}(f) = |\mathscr{A}(f)|^2 P_{x_i}(f) \tag{23}$$

has been used to obtain the right-hand relation of (22).

Define the deviations of the estimates $y_i(t)$ and $y_o(t)$ of Fig. 3 from their desired values as follows:

$$\begin{aligned} d_i(t) &\equiv y_i(t) - x_i(t) \\ d_o(t) &\equiv y_o(t) - x_o(t). \end{aligned} \tag{24}$$

The power spectra of these deviations are minimized by the optimum filters of (21) and (22), as follows:

$$\begin{aligned} P_{d_i}(f) &= \frac{P_{x_i}(f)P_\nu(f)}{|\mathscr{A}(f)|^2 P_{x_i}(f) + P_\nu(f)} \\ P_{d_o}(f) &= \frac{P_{x_o}(f)P_\nu(f)}{P_{x_o}(f) + P_\nu(f)}. \end{aligned} \tag{25}$$

The corresponding minimum mean-square deviations are obtained by integrating these spectra.

These results are applied to minimize the mean-square deviations (6) by the following substitutions in (21) through (25):

$$x_i(t) \rightarrow x_W(t)$$

$$d_i(t) \rightarrow d_W(t)$$

$$P_{x_i}(f) \rightarrow P_{x_W}(f)$$

$$H_i(f) \rightarrow H_W(f)$$

$$P_\nu(f) \rightarrow \sum_{\substack{n=-\infty \\ n\neq 0}}^{\infty} P_{x_o}\left(f - \frac{n}{T}\right) + NT. \tag{26}$$

Thus the noise $\nu(t)$ of Fig. 3 is replaced by the noise plus alias spectra of Fig. 2.[3,6] Recall that $\mathscr{A}(f) = 0$, $|f| \geq W$, and that $P_{x_o}(f)$ and $P_{x_W}(f)$ satisfy (10). Consequently, $H_W(f)$ and $H_o(f)$ both satisfy (15). The additional condition (17) eliminates all but the $n = \pm 1$ terms in the summation of the last line of (26). We summarize these results for interpolation:

$$H_o(f) = \frac{|\mathscr{A}(f)|^2}{|\mathscr{A}(f)|^2 + \left|\mathscr{A}\left(f - \frac{1}{T}\right)\right|^2 + \left|\mathscr{A}\left(f + \frac{1}{T}\right)\right|^2 + \frac{NT}{X}} \tag{27}$$

$$P_{d_o}(f) = H_o(f) \cdot X\left[\left|\mathscr{A}\left(f - \frac{1}{T}\right)\right|^2 + \left|\mathscr{A}\left(f + \frac{1}{T}\right)\right|^2 + \frac{NT}{X}\right] \tag{28}$$

and for restoration:

$$H_W(f) = \frac{1}{\mathscr{A}(f)} H_o(f) \tag{29}$$

$$\begin{aligned} P_{d_W}(f) &= \frac{P_{d_o}(f)}{|\mathscr{A}(f)|^2} \\ &= \frac{X\left[\left|\mathscr{A}\left(f - \frac{1}{T}\right)\right|^2 + \left|\mathscr{A}\left(f + \frac{1}{T}\right)\right|^2 + \frac{NT}{X}\right]}{|\mathscr{A}(f)|^2 + \left|\mathscr{A}\left(f - \frac{1}{T}\right)\right|^2 + \left|\mathscr{A}\left(f + \frac{1}{T}\right)\right|^2 + \frac{NT}{X}}. \end{aligned} \tag{30}$$

By (17), the terms $\left|\mathscr{A}\left(f - \frac{1}{T}\right)\right|^2$ and $\left|\mathscr{A}\left(f + \frac{1}{T}\right)\right|^2$ in (27), (28), and (30) never overlap. As $|f| \rightarrow W$, since $\mathscr{A}(f) \rightarrow 0$, then $H_o(f)$, $H_W(f)$, and $P_{d_o}(f)$ all $\rightarrow 0$ but $P_{d_W}(f) \rightarrow X$.

V. UNIFORM ILLUMINATION (MAXIMUM-GAIN ANTENNA)

From (2)

$$\mathscr{A}(f) = \begin{cases} 1 - |f/W|, & |f| \leq W \\ 0, & |f| \geq W. \end{cases} \tag{31}$$

We distinguish two cases:

$$0 < WT < 0.5; \quad \text{oversampled}$$

$$0.5 < WT < 1; \quad \text{undersampled.} \tag{32}$$

It is convenient to introduce an auxiliary parameter $S = \langle x_o^2(t) \rangle$ representing the total power of the quantity $x_o(t)$ at the output of the filter $\mathscr{A}(f)$ (Fig. 2); from (10)

$$S = X \int_{-W}^{W} |\mathscr{A}(f)|^2 df. \tag{33}$$

For the present maximum-gain antenna, (31) substituted into (33) yields

$$S = \frac{2}{3} XW. \tag{34}$$

Then with the substitution of (34), (27) through (30) yield, for interpolation:

$$\overline{\langle d_o^2(t) \rangle} = 2S \frac{WT}{S/N} \int_0^{\min\left(1, \frac{1}{WT} - 1\right)} \frac{(1-y)^2}{(1-y)^2 + \frac{2}{3}\frac{WT}{S/N}} dy$$

$$+ 3S \int_{\min\left(1, \frac{1}{WT} - 1\right)}^{1} \frac{(1-y)^2 \left[\left(1 + y - \frac{1}{WT}\right)^2 + \frac{2}{3}\frac{WT}{S/N}\right]}{(1-y)^2 + \left(1 + y - \frac{1}{WT}\right)^2 + \frac{2}{3}\frac{WT}{S/N}} dy, \tag{35}$$

and for restoration:

$$\overline{\langle d_W^2(t) \rangle} = 2S \frac{WT}{S/N} \int_o^{\min\left(1, \frac{1}{WT} - 1\right)} \frac{1}{(1-y)^2 + \frac{2}{3}\frac{WT}{S/N}} dy$$

$$+ 3S \int_{\min\left(1, \frac{1}{WT} - 1\right)}^{1} \frac{\left(1 + y - \frac{1}{WT}\right)^2 + \frac{2}{3}\frac{WT}{S/N}}{(1-y)^2 + \left(1 + y - \frac{1}{WT}\right)^2 + \frac{2}{3}\frac{WT}{S/N}} dy. \tag{36}$$

Here we combine the two cases of (32). S/N is the observed signal-to-noise power of the samples in Fig. 2, and WT is the parameter bounded by (32), indicating the relative degree of over- or undersampling and

consequent aliasing. The first terms of (35) and (36) consist of noise and distortion. In the oversampled case the second terms are zero; in the undersampled case the second terms contain aliasing as well.

While it is possible to evaluate (35) and (36) in closed form, the results are messy. Moreover, such evaluations for other more realistic antenna patterns than the present uniform illumination (e.g., the truncated Gaussian illumination considered in the following section) will be worse in this regard. Consequently, these integrals have been evaluated numerically, with results given in Figs. 4 and 5, showing the average deviation power versus sampling parameter for interpolation and for restoration, respectively, with observed signal-to-noise ratio as a parameter. We note that the deviation is worse for restoration than for interpolation, because in the former case we attempt to equalize the input filter $\mathscr{A}(f)$, thereby enhancing the noise. Alternatively, Figs. 4 and 5 may be obtained by direct numerical integration of (18), using (6), (19), (27), and (29). Analytical expressions for these results in the oversampled case, $0 < WT < 0.5$, are given in eqs. (77) and (78) of Appendix C.

For the undersampled case, $WT > 0.5$, we require in addition the ac component of the deviation powers. We write

$$\langle d_o^2(t) \rangle \equiv \overline{\langle d_o^2(t) \rangle} - D_o \cos 2\pi \frac{t}{T}, \tag{37}$$

where D_o and D_W are the amplitudes of the ac components of the deviation powers for interpolation and for restoration, respectively.

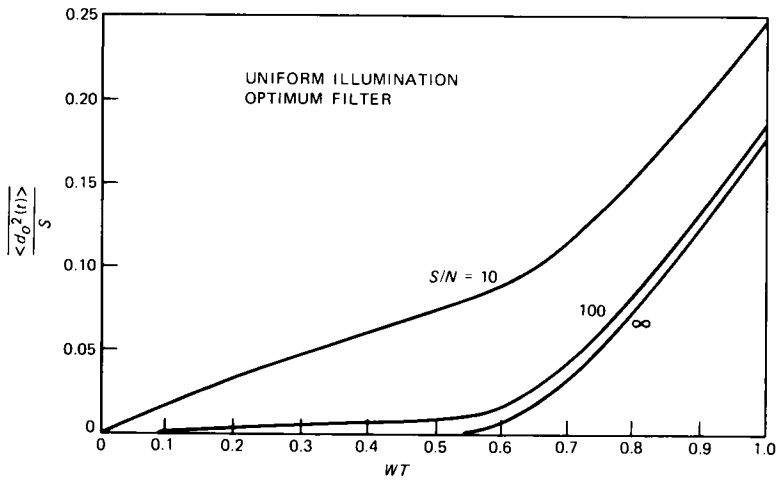

Fig. 4—Average deviation power versus sampling parameter, with signal-to-noise ratio as a parameter, for interpolation of a bandlimited function: uniform illumination and optimum filter.

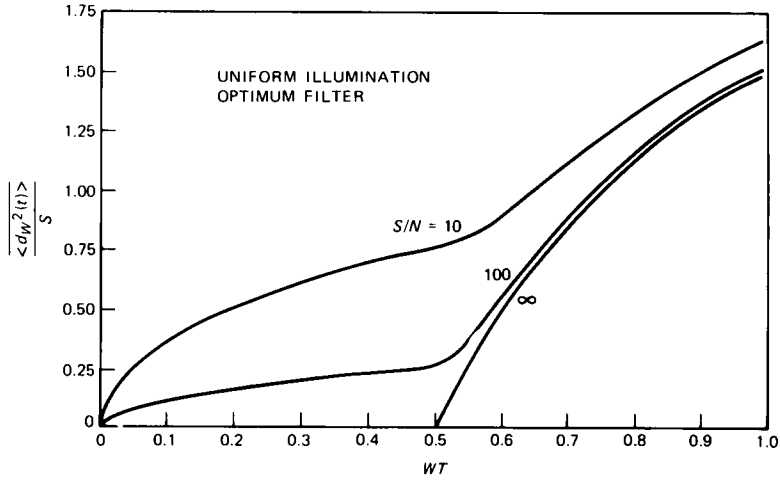

Fig. 5—Average deviation power versus sampling parameter, with signal-to-noise ratio as a parameter, for restoration of a bandlimited function: uniform illumination and optimum filter.

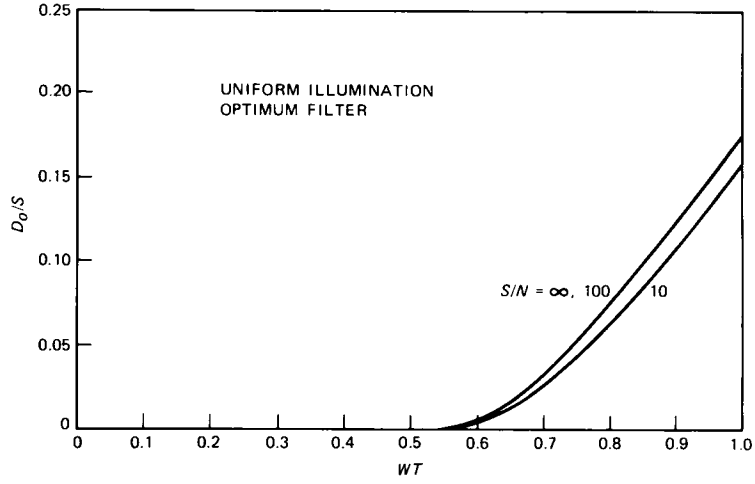

Fig. 6—Diagram of ac deviation power versus sampling parameter, with signal-to-noise ratio as a parameter, for interpolation of a bandlimited function: uniform illumination and optimum filter.

We determine D_o and D_W from this definition (37) by combining (6), (18) through (20), (27), and (29). Numerical integration of the resulting expressions yields the results shown in Figs. 6 and 7.

A partial check on these results is obtained by observing that for zero noise optimum interpolation must recover the filtered input with zero error at the sample points, i.e., $x_o(nT)$ must be reconstructed

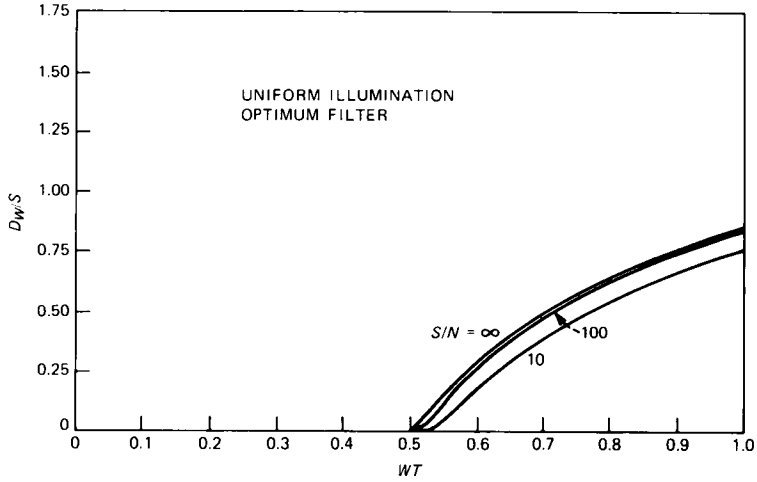

Fig. 7—Diagram of ac deviation power versus sampling parameter, with signal-to-noise ratio as a parameter, for restoration of a bandlimited function: uniform illumination and optimum filter.

without error for $N = 0$. Consequently, the $S/N = \infty$ curves of Fig. 4 and Fig. 6 must coincide, and they do.

Observe that while $H_o(f)$ of (27), the optimum filter for interpolation, decreases monotonically as f goes from 0 to W, the same is not true for $H_W(f)$. In contrast $H_W(f)$, the optimum filter for restoration, initially increases to a maximum before finally dropping to zero at $f = W$. For example, consider the oversampled case, $WT < 0.5$. Then

$$H_W(f) = \frac{1 - \dfrac{f}{W}}{\left(1 - \dfrac{f}{W}\right)^2 + \dfrac{2}{3}\dfrac{WT}{S/N}}. \tag{38}$$

Obviously,

$$H_W(0) = \frac{1}{1 + \dfrac{2}{3}\dfrac{WT}{S/N}}; \qquad H_W(W) = 0. \tag{39}$$

The peak is given by

$$H_W(f)\,|_{\max} = 0.5\sqrt{\frac{3}{2}\frac{S/N}{WT}} \quad \text{at} \quad \frac{f}{W} = 1 - \sqrt{\frac{2}{3}\frac{WT}{S/N}}. \tag{40}$$

For large S/N the peak of $H_W(f)$ is very large, and very close to $f = W$. However, the results of Fig. 5 and 7 remain finite as $S/N \to \infty$.

D_o and D_W of (37) contain contributions from the second and first

equations of (18), respectively, and from the third equation of (18), used together with (20). The former consist of linear distortion and aliasing, the latter of noise. All such contributions (to the ac coefficients D) are 0 for the oversampled case, $WT < 0.5$. For the undersampled case, $0.5 < WT < 1$, distortion and aliasing make positive contributions to D_o and D_W, while noise makes negative contributions to these quantities. Taking note of the negative sign on the last term in (37), the deviation due to distortion and aliasing is worst between the sample points, while the deviation due to noise is worst at the sample points.

The deviation powers in Figs. 4 through 7 have been normalized to the signal power at the output of $\mathscr{H}(f)$ in Fig. 2a, $S \equiv \langle x_o^2(t) \rangle$, given for the present case by (34). This is perfectly appropriate for Figs. 4 and 6 ("interpolation"), where we wish to reconstruct the quantity $x_o(t)$. It is less appropriate for restoration, where we wish to reconstruct $x_W(t)$, the bandlimited version of the input $x(t)$ in Fig. 2a, given by (4). Here a more appropriate normalization might be the total power of $x_W(t)$. For the present case (31), (10) and (34) yield

$$\langle x_W^2(t) \rangle = 2XW = 3S. \tag{41}$$

To normalize Figs. 5 and 7 ("restoration") in this way, simply divide the numbers on the vertical axes by 3 and relabel these axes accordingly.

The parameter S/N of Figs. 4 through 7 is appropriate for both interpolation and restoration, since it is the signal-to-noise ratio observed at the sampled output of a radiometer used to measure incoherent fields. However, observe that S/N defined here, and used throughout the remainder of this paper, is different than the conventional signal-to-noise ratio at the output of a radiometer receiver. In the present work S is proportional to the *fluctuation* in the radiometer signal output as the antenna is scanned across the sky; while the conventional radiometer signal output is taken as the average signal output as the antenna is scanned across the sky. As we noted in Section II, we assume the average radio brightness is deterministic, and we treat it separately (see Appendix A).

VI. GAUSSIAN ILLUMINATION

Let a one-dimensional antenna of width W have an aperture field that is Gaussian:

$$E(x) = \begin{cases} e^{-0.2 \ln 10 \cdot d \cdot \left(\frac{x}{W}\right)^2}, & |x| < \frac{W}{2} \\ 0, & |x| > \frac{W}{2}. \end{cases} \tag{42}$$

The field at the edge of the aperture is d dB down from the maximum field (at the center of the aperture);

$$d = -20 \log_{10} E\left(\frac{W}{2}\right). \tag{43}$$

The symbol d represents the aperture "taper".

$\mathscr{A}(f)$ of (3) and Fig. 2, the Fourier transform of the effective width $A(t)$ of the antenna, is proportional to the convolution of $E(f)$ of (42) with itself; by (1)

$$\mathscr{A}(f) = \frac{\int_{\max\left(-\frac{W}{2}, -\frac{W}{2}+f\right)}^{\min\left(\frac{W}{2}, \frac{W}{2}+f\right)} E(x)E(x-f)dx}{\int_{-\frac{W}{2}}^{\frac{W}{2}} E^2(x)dx}. \tag{44}$$

For $d = 0$, (42) substituted into (44) yields (31) of the preceding section for uniform illumination.

Figures 8 through 11 give the average and ac deviation powers versus sampling parameter with signal-to-noise ratio as a parameter, for interpolation and for restoration, for Gaussian aperture illumination with taper $d = 15$ dB. These results may be compared with Figs. 4 through 7, respectively, for uniform illumination, treated in the preceding section. As in this prior case, numerical integration seems

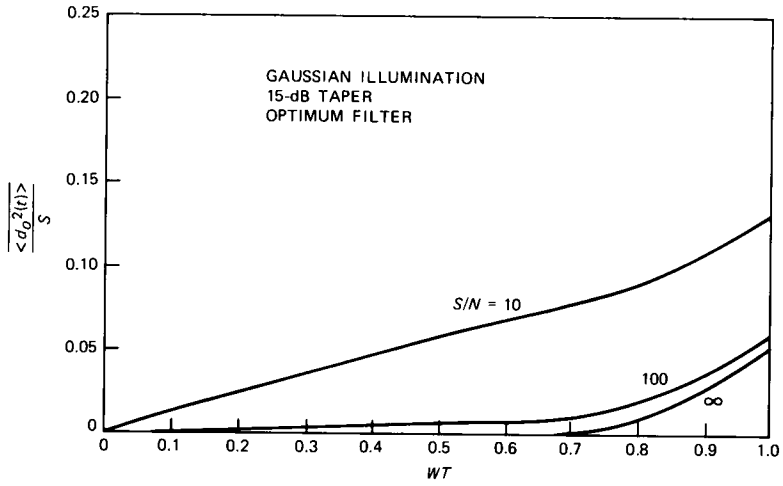

Fig. 8—Average deviation power versus sampling parameter, with signal-to-noise ratio as a parameter, for interpolation of a bandlimited function: Gaussian illumination with 15-dB taper, optimum filter.

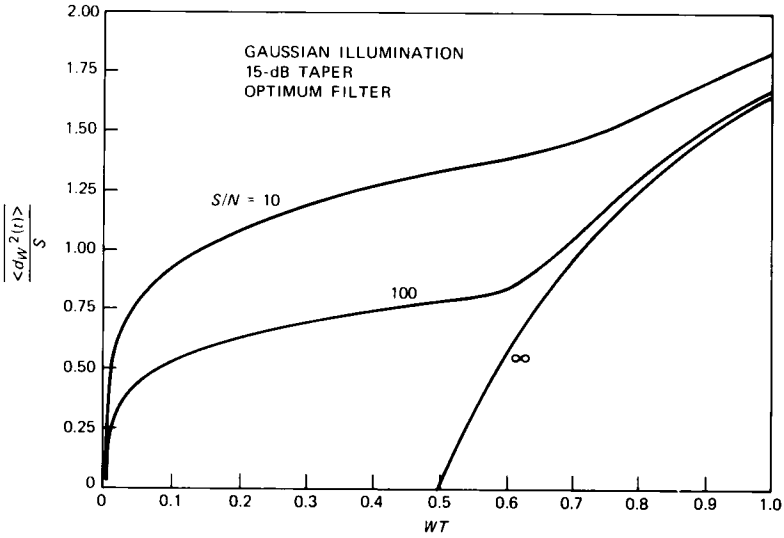

Fig. 9—Average deviation power versus sampling parameter, with signal-to-noise ratio as a parameter, for restoration of a bandlimited function: Gaussian illumination with 15-dB taper, optimum filter.

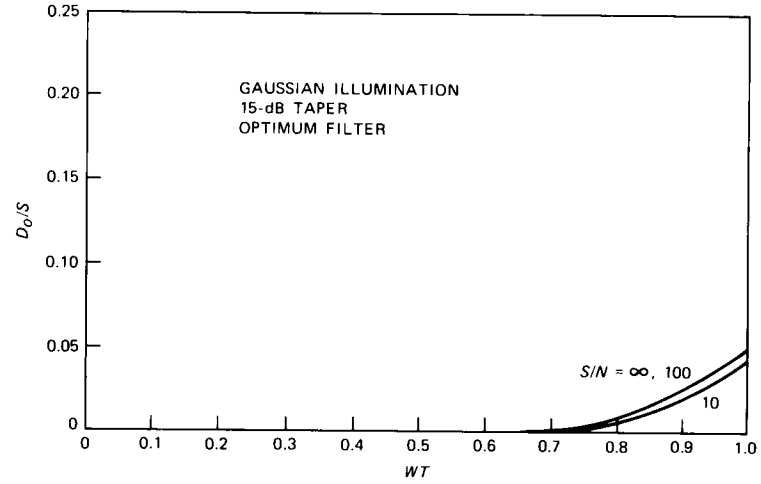

Fig. 10—Diagram of ac deviation power versus sampling parameter, with signal-to-noise ratio as a parameter, for interpolation of a bandlimited function: Gaussian illumination with 15-dB taper, optimum filter.

preferable to analytical treatment. Equation (44) is evaluated using (42), the results substituted into (27), (29), and (18), and finally (6) and (37) are evaluated using (19) and (20).

Much of the discussion of the preceding section for uniform illumination applies also to the present Gaussian case. For zero noise the

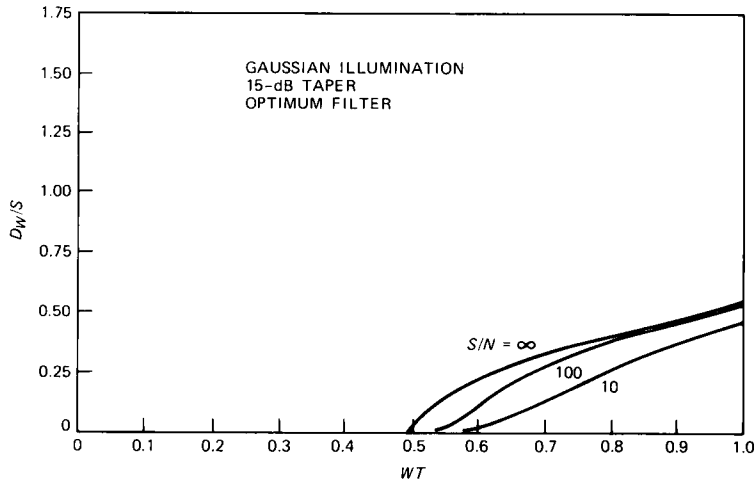

Fig. 11—Diagram of ac deviation power versus sampling parameter, with signal-to-noise ratio as a parameter, for restoration of a bandlimited function: Gaussian illumination with 15-dB taper, optimum filter.

$S/N = \infty$ curves of Figs. 8 and 10 again coincide. To normalize the "restoration" results to the total power of $x_W(t)$ (rather than to $S \equiv \langle x_o^2(t) \rangle$), (10) and (42), (44) yield

$$\langle x_W^2(t) \rangle = 2xW = 3.281S, \qquad d = 15 \text{ dB}; \tag{45}$$

simply divide the numbers on the vertical axes of Figs. 9 and 11 by 3.281 and relabel these axes accordingly.

An important difference between the results for uniform illumination (discussed in the preceding section) and the present results for the more practical Gaussian illumination with 15-dB taper appears in the "restoration" results of Figs. 5 and 9 for these two cases, respectively. Restoration is much more difficult in the present case because the input filter $\mathscr{A}(f)$ in Fig. 2 falls off much faster with f, requiring greater equalization by the output filter and hence yielding more output noise.

VII. SUBOPTIMUM FILTERS

We have so far considered only optimum reconstruction filters, according to Section IV, for both interpolation and for restoration. Such filters must be changed for each different signal-to-noise ratio S/N. We now explore the use of *fixed* filters, for interpolation and for restoration, which are independent of S/N.

Consider interpolation first. The optimum filter $H_o(f)$ of (27) is well behaved and, in particular, changes only slightly as the noise power N

increases from zero. It is natural to use $H_o(f)$ for $N = 0$ as a suboptimum filter for finite but small N, i.e., for large but finite S/N.

The situation for restoration is quite different. The optimum filter $H_W(f)$ of (29) is badly behaved, as we discussed in connection with (38) through (40); small changes in S/N can produce large changes in $H_W(f)$ near its peak. For the oversampled case, $0 < WT < 0.5$, $H_W(f)$ for $N = 0$ has a pole at $f = W$, and this filter therefore yields infinite output noise for finite S/N. Consequently, use of $H_W(f)$ for $N = 0$ for finite S/N is restricted to the undersampled case, $0.5 < WT < 1$.

Figures 12 through 15 show the average deviation power for interpolation and for restoration, for uniform illumination and for Gaussian illumination with a 15-dB taper. In all cases the suboptimum filter used is the optimum filter for $S/N = \infty$. For restoration, only the undersampled case, $0.5 < WT < 1$, is shown, as we discussed above.

Observe that the curves of Figs. 12 and 14 (suboptimum interpolation, for uniform and for Gaussian illumination, respectively) are identical in the oversampled case, $0 < WT < 0.5$. Here the reconstruction filter is simply

$$H(f) = \begin{cases} 1, & |f| < W \\ 0, & |f| > W. \end{cases} \tag{46}$$

Thus, since aliasing is absent, in the absence of noise the suboptimum

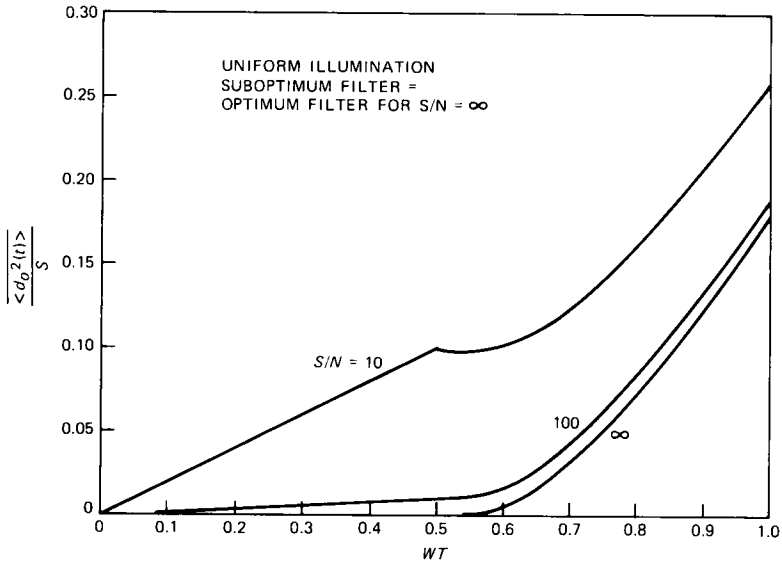

Fig. 12—Average deviation power versus sampling parameter, with signal-to-noise ratio as a parameter, for interpolation of a bandlimited function: uniform illumination, suboptimum filter equal to optimum filters for $S/N = \infty$.

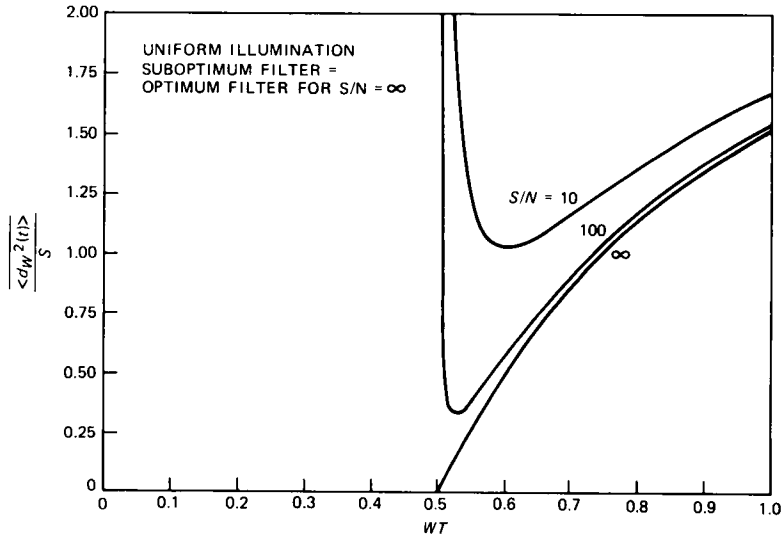

Fig. 13—Average deviation power versus sampling parameter, with signal-to-noise ratio as a parameter, for restoration of a bandlimited function: uniform illumination, suboptimum filter equal to the optimum filter for $S/N = \infty$.

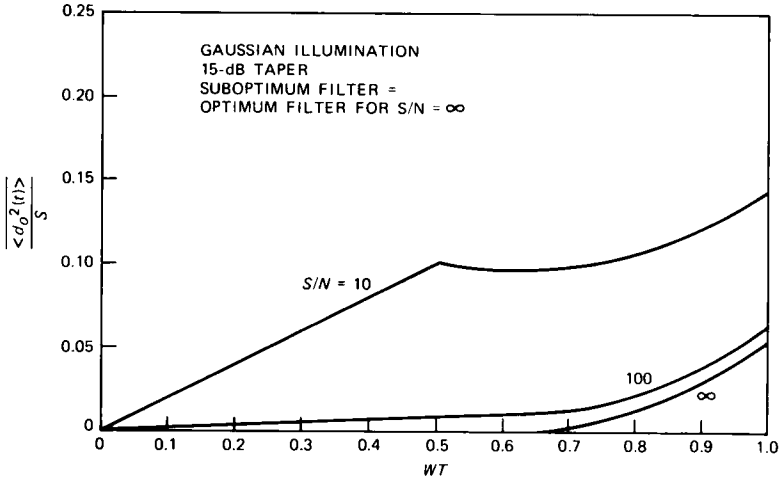

Fig. 14—Average deviation power versus sampling parameter, with signal-to-noise ratio as a parameter, for interpolation of a bandlimited function: Gaussian illumination with 15-dB taper, suboptimum filter equal to optimum filter for $S/N = \infty$.

(i.e., zero noise) reconstruction filter simply passes the input without distortion. The output deviation then results from noise alone. A simple result is given in (79), Appendix C, for this case. We can observe further comparing (77) and (79) that the $S/N = 10$ curves in Figs. 4 and 12 start out with identical slope for small WT, but that as

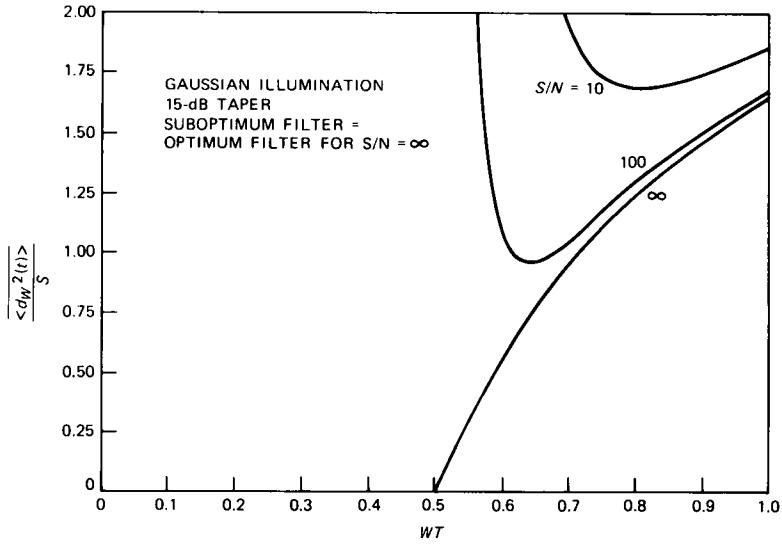

Fig. 15—Average deviation power versus sampling parameter, with signal-to-noise ratio as a parameter for restoration of a bandlimited function: Gaussian illumination with 15-dB taper, suboptimum filter equal to optimum filter for $S/N = \infty$.

WT increases the curve of Fig. 4, for the optimum interpolation filter, falls below the curve of Fig. 12, for the suboptimum interpolation filter.

We conclude that for interpolation with large S/N, we may use the reconstruction filter designed for $S/N = \infty$ with little loss. This is *not* true for restoration. These results are to be expected from the discussion of the optimum filters given above in these two cases. The ac deviation powers for interpolation do not change much from those of Figs. 6 and 10, so we omit plots of them here.

For interpolation with smaller S/N, the greatest penalty for the suboptimum filter occurs near critical sampling, $WT = 0.5$. For example, compare Figs. 4 and 8 with Figs. 12 and 14, respectively, for $S/N = 10$; the suboptimum filter is about 35 percent worse for uniform illumination and about 67 percent worse for Gaussian illumination with a 15-dB taper than the optimum filters for these cases.

VIII. DISCUSSION

The present results show how to process data obtained by measurement of a one-dimensional incoherent field with a one-dimensional antenna, and what the resulting errors will be. We assume the present results provide some indication for the real, two-dimensional case.

In the model of Fig. 2, T is the sampling interval and N is the noise power. By the definitions in Section II, T corresponds to the angular

separation between antenna observations, and N to the mean-square error in receiver output due to receiver noise. The noise of a radiometer receiver is inversely proportional to the observation time;[1] moreover, if a given time is allotted to measure a given region of the sky, the time per observation is inversely proportional to the number of observations, or directly proportional to the angular separation between observations. Consequently,

$$NT = \frac{\text{Constant}}{\text{Observing Time per Unit Angle of Sky}}, \tag{47}$$

where the constant in (47) is independent of the antenna.

Let us examine the data of Figs. 4, 5, 8, 9, 12, or 14 for fixed observing time per unit angle, i.e., from (47) for NT = constant. Consider as a specific example Fig. 4. Take the point given by $S/N = 100$, $WT = 1$; then $\overline{\langle d_o^2(t)\rangle}/S \approx 0.187$. The measurement parameters $S/N = 10$, $WT = 0.1$ yield the same value of NT, and hence by (47) the same observing time per unit angle of sky; for these parameters $\overline{\langle d_o^2(t)\rangle}/S \approx 0.017$. In this example, sampling ten times as often with 1/10 the signal-to-noise ratio has reduced the mean-square deviation by a factor of $0.187/0.017 \approx 11$. More generally, for average deviation in any of the above figures, compare:

1. Any $S/N = 10$ curve.
2. The corresponding $S/N = 100$ curve with its horizontal scale compressed by a factor of 10, i.e., each point x, y replotted to $x/10$, y.

In every case the compressed $S/N = 100$ curve will lie above the $S/N = 10$ curve for $WT > 0.05$. For $0 \leq WT \leq 0.05$ the two curves coincide precisely, as we see in the second paragraph of Appendix C.

From this, we conclude that undersampling is *always* bad; it will always be better to reduce T and increase N, i.e., to take more closely spaced observations each with poorer signal-to-noise ratio, to avoid operating in the undersampled region. Moreover, in the preferred oversampled region the family of curves in each of these figures can be combined into a single curve; i.e., for $0 \leq WT \leq 0.5$ the mean-square deviation $\overline{\langle d^2(t)\rangle}/S$ is a function of the single normalized variable $[(S/N)/(2WT)]$. These results are in agreement with a prior observation of R. W. Wilson.

Recalling from Section VII that Figs. 12 and 14 are identical for $0 \leq WT \leq 0.5$, only five curves are required to summarize the data of Figs. 4, 5, 8, 9, 12, and 14 in the oversampled region. This is done in Figs. 16 and 17, for interpolation and for restoration, respectively. Note that the vertical axis of Fig. 16 has been normalized to $S \equiv \langle x_o^2(t)\rangle$ of (33), the same as Figs. 4, 8, 12, and 14. However, the vertical axis of Fig. 17 has rather been normalized to $\langle x_W^2(t)\rangle$, as discussed in

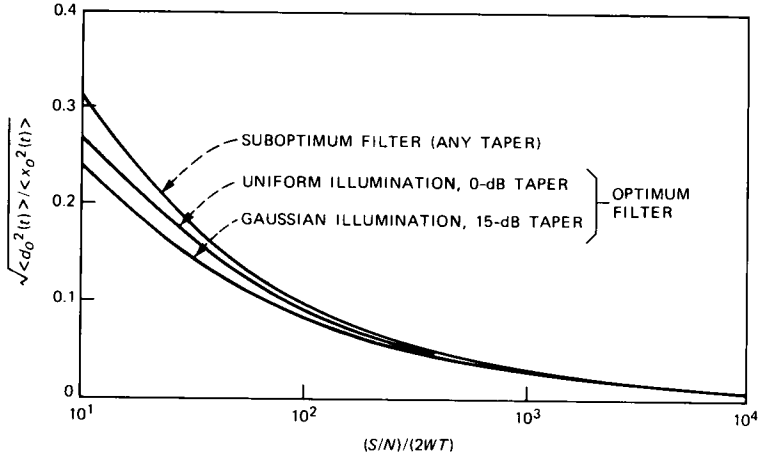

Fig. 16—Root-mean-square deviation for interpolation versus signal-to-noise ratio in the oversampled case, $0 \leq WT \leq 0.5$.

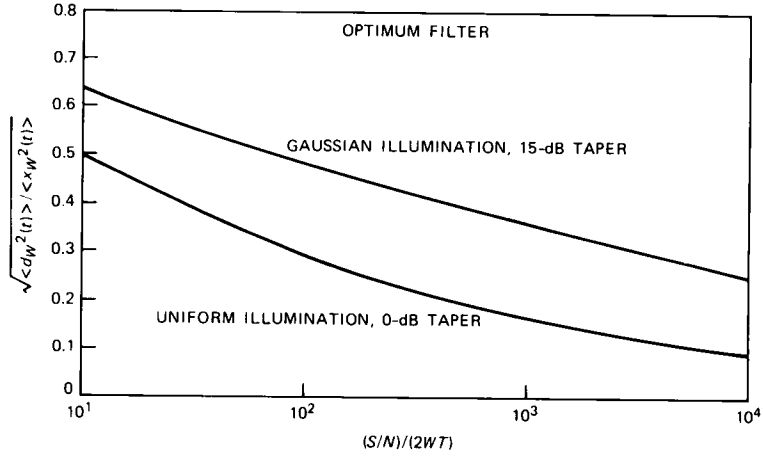

Fig. 17—Root-mean-square deviation for restoration versus signal-to-noise ratio in the oversampled case, $0 \leq WT \leq 0.5$.

(41) and (45), i.e., different than the normalization for Figs. 5 and 9. For a given antenna and a given receiver noise temperature, the total observing time for a given area of sky is proportional to the product of the area observed and the horizontal axis variable $[(S/N)/(2WT)]$ of Figs. 16 and 17; however, observe from (33) and (47) that the constant of proportionality depends on the antenna illumination, and hence differs for the uniform and for the Gaussian cases.

Finally, we observe that while undersampling ($WT > 0.5$) is bad, oversampling ($WT < 0.5$) offers no advantage over critical sampling

($WT = 0.5$). Reducing WT below 0.5 requires more data storage, with no reduction in error.

Let us examine the implications of these results for ordinary antennas. Consider the antenna of Section VI, with Gaussian illumination (42) and significant taper (e.g., $d = 15$ dB, as in the examples). To determine the gross structure of the main lobe we may neglect the truncation of the aperture field in (42), i.e., assume $E(x)$ is given by the top expression of (42) for all x. Then the effective width is the Fourier transform of (44) with infinite limits on the integrals:

$$A(t) \approx W \sqrt{\frac{10\pi}{d \ln 10}}\, e^{-\frac{10}{d \ln 10}(\pi Wt)^2}, \qquad Wt < \sqrt{\frac{d}{10}}; \quad d \gg 1. \tag{48}$$

Observations are frequently taken at an angular separation of one full 3-dB beamwidth; i.e., the receiving power patterns at two adjacent observations overlap at their 3-dB points. In our present model this corresponds to a sampling interval

$$T = 2t_{3\text{-dB}}, \tag{49}$$

where $t_{3\text{-dB}}$ is the 3-dB half-width of the antenna pattern (48);

$$A(t_{3\text{-dB}}) = \frac{1}{2} \cdot A(0). \tag{50}$$

From (48) through (50)

$$W \cdot 2t_{3\text{-dB}} = \frac{1}{\pi} \sqrt{\frac{d \ln 10 \ln 2}{10}}. \tag{51}$$

For the 15-dB taper chosen for the examples, (51) yields

$$W \cdot 2t_{3\text{-dB}} = 0.985, \qquad d = 15\text{-dB taper}. \tag{52}$$

Thus, measurements separated by a full 3-dB beamwidth with a 15-dB antenna taper will be undersampled by about a factor of 2, with corresponding penalties indicated in Figs. 8 and 9.

Table I illustrates the above discussion. The same antenna size and

Table I—Numerical examples

WT	$10 \log_{10} S/N$ (dB)	d (dB)	Normalized Observing Time	Normalized rms Deviations					
				Interpolation			Restoration		
				Avg.	Max.	Min.	Avg.	Max.	Min.
1.0	20	15	1	0.24	0.33	0.095	0.72	0.83	0.60
0.5	17	15	1	0.12	0.12	0.12	0.53	0.53	0.53
0.5	57	15	10,000				0.12	0.12	0.12
0.5	36	0	73				0.12	0.12	0.12

receiver noise figure are assumed for the four cases shown. A typical antenna, with Gaussian illumination and a 15-dB taper, is used for the first three examples. The final example uses a maximum-gain antenna, with uniform illumination (no taper). The root-mean-square (rms) deviations have been normalized to $\langle x_o^2(t)\rangle = S$ for interpolation (33) and to $\langle x_W^2(t)\rangle = 2XW$ for restoration (41), (45). In each case, from (47)

$$\text{Observing Time} = \frac{\text{Constant}}{NT} = \text{Constant}\cdot\frac{W}{S}\cdot\frac{S/N}{WT}, \tag{53}$$

with the third factor determined from the first and second columns of the above table, and S in the denominator of the second factor given by (45) for the first three examples and by (41) for the last example. Finally, the observing times are normalized such that the first two examples have normalized observing times equal to unity.

In the top row observations are taken at twice critical separation (i.e., observations separated by about a full 3-dB beamwidth). Since the data are undersampled, the rms deviations vary, being minimum at the observation points and maximum half-way in between. The normalized deviation is much larger for restoration than for interpolation.

The second row shows the same antenna and receiver with critical sampling. Twice as many observations are made, each for half the time, with the signal-to-noise ratio reduced by 3 dB; hence, the total observing time for a given area of the sky is the same as for the first row. The rms deviations are now independent of position with respect to the observation points. The rms interpolation deviation is about half as large, and the rms restoration deviation is about three-fourths as large, as the corresponding average deviations for the undersampled case, in row 1. The deviation for restoration remains much larger than that for interpolation.

The third row shows the same antenna and receiver as the first two rows, with a 40-dB higher signal-to-noise ratio than the second row; consequently, the total observing time is increased by a factor of 10,000. The deviations are greatly reduced, that for restoration now being equal to the interpolation deviation for the preceding case of row 2.

Finally, the fourth row shows that a maximum-gain antenna, with uniform illumination (no taper), and the same receiver as that of row 3, will attain the same rms restoration deviation with a total observing time of only 73, as compared to 10,000 for an antenna with Gaussian illumination and a 15-dB taper (row 3). Of course, the observing time is still large compared to that of row 2; i.e., to obtain the same rms deviation for restoration with an antenna with uniform illumination

as for interpolation with an antenna with a 15-dB taper takes 73 times as long.

The above discussion makes undersampling appear unattractive. Nevertheless, much existing data have been taken in this way; the present results show the best way to process such data, and the resulting errors. The optimum filters (27) and (29) in the undersampled case minimize the time-average mean-square deviations $\overline{\langle d^2(t) \rangle}$ in the present model (6). It is shown in Appendix D that they also minimize the time-dependent mean-square deviations $\langle d^2(t) \rangle$. In the corresponding antenna problem the optimum data spatial filters minimize the mean-square error everywhere in the region containing the observed points.

IX. CONCLUSIONS

Consider astronomical measurements of radio brightness that has white spatial variation (i.e., that varies rapidly compared to the beamwidth of the antenna used to make the measurement), made at a regular array of points in the sky. Optimum mean-square estimates for the measured and true brightness at any point in the sky are called "interpolation" and "restoration", respectively. Idealize this problem to one dimension. Then:

1. Data points should be separated by about half the (full) 3-dB beamwidth for a normal antenna, having a tapered aperture illumination; i.e., the receiving power patterns at two adjacent observations should overlap at their 0.75-dB points. This is often not done.

2. Interpolation can be accomplished with reasonable accuracy and reasonable observation time.

3. Restoration with reasonable accuracy requires much longer observation time than interpolation.

4. Optimum spatial filters depend on the signal-to-noise ratio. For interpolation this dependence is very weak. The optimum filter for zero noise works fairly well for interpolation of finite signal-to-noise ratios; this is not true for restoration.

5. A maximum-gain antenna, with uniform aperture illumination, is better for restoration than a conventional antenna with tapered aperture illumination.

The following additional studies are suggested by the present work:

1. Interpolation and restoration with a finite number of data points, perhaps not regularly spaced (e.g., edge effects).

2. Tolerances in the spatial filters applied to the measured data, and in the antenna illumination.

3. Interpolation and restoration with reduced resolution, by additional spatial filtering.

4. Nonwhite sky brightness statistics, e.g., strong isolated point sources embedded in white brightness.

5. Treatment of the real two-dimensional problem. Greater variety is evident, e.g., square, hexagonal, and irregular sampling patterns are of interest in two dimensions.

X. ACKNOWLEDGMENT

I would like to thank R. W. Wilson for suggesting this problem and for many helpful discussions, T. S. Chu for suggesting the study of restoration with reduced resolution, L. J. Greenstein for helpful discussions of the equivalent sampled-data system and Ref. 3, R. E. Hills for suggesting the study of the maximum-gain antenna, and M. J. Gans, M. Kavehrad, and J. Minkoff for careful reviews of this paper.

REFERENCES

1. H. E. Rowe, "Processing Channel-Bank Spectrometer Data," AT&T Bell Lab. Tech. J., *63*, No. 4 (April 1984), pp. 565–85.
2. R. N. Bracewell, "Two-Dimensional Aerial Smoothing in Radio Astronomy," Australian J. Phys., *9* (September 1956), pp. 297–314.
3. K. W. Cattermole, *Principles of Pulse Code Modulation*, New York: American Elsevier, 1969, pp. 44–64.
4. H. E. Rowe, *Signals and Noise in Communications Systems*, New York: Van Nostrand Reinhold, 1965, p. 244.
5. A. Papoulis, *Probability, Random Variables, and Stochastic Processes*, New York: McGraw-Hill, 1965, pp. 400–7.
6. J. W. Brault and O. R. White, "The Analysis and Restoration of Astronomical Data via the Fast Fourier Transform," Astron. Astrophys., *13* (July 1971), pp. 169–89 (see pp. 183–6).
7. Ref. 4, pp. 41–3.
8. Ref. 5, pp. 390–400.

APPENDIX A

Condition for DC Component To Be Deterministic

A real wide-sense stationary random process has mean $\langle x(t) \rangle$ and covariance $\phi_x(\tau) \equiv \langle x(t+\tau)x(t) \rangle$, both independent of t. We assume

$$\lim_{|\tau| \to \infty} \phi_x(\tau) = a^2. \tag{54}$$

Then define $\phi_{x_c}(\tau)$ by the relation

$$\phi_x(\tau) \equiv a^2 + \phi_{x_c}(\tau). \tag{55}$$

Thus,

$$\lim_{|\tau| \to \infty} \phi_{x_c}(\tau) = 0. \tag{56}$$

The spectral density $P_x(f)$, the Fourier transform of $\phi_x(\tau)$, is by (55)

$$P_x(f) = a^2\delta(f) + P_{x_c}(f), \tag{57}$$

where $P_{x_c}(f)$ is the Fourier transform of $\phi_{x_c}(\tau)$ of (55). By (56), $P_{x_c}(f)$ contains no component proportional to $\delta(f)$, i.e., $P_{x_c}(f)$ contains no delta function at the origin. The dc power of $x(t)$ is thus a^2.

Now define

$$\overline{x(t)} \equiv \lim_{T\to\infty} \frac{1}{2T} \int_{-T}^{T} x(t)dt \tag{58}$$

as the dc component of an individual noise wave $x(t)$. We have

$$\langle \overline{x(t)} \rangle = \langle x(t) \rangle. \tag{59}$$

Next,

$$\langle \overline{x(t)}^2 \rangle = \lim_{T\to\infty} \frac{1}{(2T)^2} \int_{-T}^{T} \int_{-T}^{T} \phi_x(t-s)dt\, ds = a^2. \tag{60}$$

Define $x_{ac}(t)$ by the relation

$$x(t) \equiv \overline{x(t)} + x_{ac}(t). \tag{61}$$

Then

$$\langle x_{ac}(t) \rangle = 0, \tag{62}$$

$$\phi_x(\tau) = a^2 + \phi_{x_{ac}}(\tau). \tag{63}$$

If we compare (55) and (63),

$$\phi_{x_{ac}}(\tau) = \phi_{x_c}(\tau). \tag{64}$$

We investigate the conditions under which $\overline{x(t)} = \langle x(t) \rangle$ with probability 1, i.e., for which almost every $x(t)$ has the same dc component. Define

$$y \equiv \overline{x(t)} - \langle x(t) \rangle. \tag{65}$$

Obviously $\langle y \rangle = 0$. Now,

$$\langle y^2 \rangle = \langle \overline{x(t)}^2 \rangle - \langle x(t) \rangle^2 = a^2 - \langle x(t) \rangle^2, \tag{66}$$

the last step following from (60).

Therefore, if

$$\lim_{|\tau|\to\infty} \phi_x(\tau) = \langle x(t) \rangle^2, \tag{67}$$

then with probability 1

$$\overline{x(t)} \equiv \lim_{T\to\infty} \frac{1}{2T} \int_{-T}^{T} x(t)dt = \langle x(t) \rangle. \tag{68}$$

The dc component may then be treated as a fixed quantity, and the ac component [whose spectrum is the second term of (57)] estimated

separately. A stationary shot noise, for example, satisfies (67). Note that in (67)

$$\lim_{|\tau|\to\infty} \phi_x(\tau) = \lim_{\epsilon\to 0} \int_{-\epsilon}^{\epsilon} P_x(f)df. \tag{69}$$

APPENDIX B

Derivation Of Time-Varying Deviations

The time average of the expected error powers (5) and noise power are given immediately in terms of their power spectra, (9) and (12), by (11) and (13). However, the time-varying error and noise powers (18) are not so easily obtained. All three quantities of (18) are derived in a similar manner; we choose the middle one, $\langle e_o^2(t)\rangle$, as representative.

Use the Fourier series representation for the random process $x_o(t)$, as follows:[7]

$$x_o(t) = \sum_{|n|<N} x_{on} e^{jn2\pi f_0 t} \tag{70}$$

$$N \equiv \frac{W}{f_0} \tag{71}$$

$$\lim_{f_0\to 0} \frac{1}{f_0} \langle x_{on} x_{om}^* \rangle = 0, \qquad n \neq m. \tag{72}$$

$$\lim_{f_0\to 0} \frac{1}{f_0} \langle |x_{on}|^2 \rangle = P_{x_o}(nf_0). \tag{73}$$

The restriction on the summation in (70), with N defined in (71), arises from (14). From Fig. 2, the error $e_o(t)$ of (5) is given by

$$\begin{aligned} e_o(t) = &\sum_{|n|<N} (H_n - 1) x_{on} e^{jn2\pi f_0 t} \\ &+ e^{j2\pi \frac{t}{T}} \sum_{-N<n<0} H_{n+K} x_{on} e^{jn2\pi f_0 t} \\ &+ e^{-j2\pi \frac{t}{T}} \sum_{0<n<N} H_{n-K} x_{on} e^{jn2\pi f_0 t}, \end{aligned} \tag{74}$$

where

$$H_n \equiv H(nf_0), \qquad K \equiv \frac{1}{f_0 T}. \tag{75}$$

The restrictions on the summations in (74) arise from (14), (15), and

(17). The first line of (74) represents linear distortion; the second and third lines represent aliasing. If we combine terms in (74),

$$e_o(t) = \sum_{-N<n<0} [e^{j2\pi \frac{t}{T}} H_{n+K} - 1 + H_n] x_{on} e^{jn2\pi f_0 t} + \sum_{0<n<N} [e^{-j2\pi \frac{t}{T}} H_{n-K} - 1 + H_n] x_{on} e^{jn2\pi f_0 t}, \quad (76)$$

where we ignore the $n = 0$ term by the assumption that any dc component is deterministic and treated separately. Calculating $\langle e_o^2(t) \rangle$ using (72) and (73), we obtain the middle relation of (18). The other two relations are similarly obtained.

APPENDIX C

Some Analytical Results

Consider the results (35) and (36) for a one-dimensional antenna with uniform illumination in the oversampled case, $0 < WT < 0.5$. Here $\min(1, 1/(WT) - 1) = 1$; aliasing is absent, the upper limit of the first terms in (35) and (36) is 1, and the second terms in these relations are absent. Then these results are readily evaluated by partial fraction expansions of the integrands to yield the following results for optimum reconstruction filters, for interpolation and for restoration, respectively:

$$\langle d_o^2(t) \rangle = 2S \frac{WT}{S/N} \left[1 - \sqrt{\frac{2}{3} \frac{WT}{S/N}} \tan^{-1} \sqrt{\frac{3}{2} \frac{S/N}{WT}} \right] \quad (77)$$

and

$$\langle d_W^2(t) \rangle = 3S \sqrt{\frac{2}{3} \frac{WT}{S/N}} \tan^{-1} \sqrt{\frac{3}{2} \frac{S/N}{WT}}. \quad (78)$$

These relations give the curves of Figs. 4 and 5 for $0 < WT < 0.5$. We omit similar, but messier, results for $0.5 < WT < 1$. Observe that the normalized deviations (77) and (78) are functions of only $(WT)/(S/N)$. In the oversampled case we can reduce the sampling interval and signal-to-noise ratio proportionately; i.e., in Figs. 4 and 5 for $0 < WT < 0.5$, the points with equal y-coordinates on the $S/N = 100$ and $S/N = 10$ curves have x-coordinates WT whose ratio is precisely 10. This simple property does not hold if either x-coordinate $WT > 0.5$.

We have no such analytic results for Gaussian illumination, Figs. 8 and 9. However, R. W. Wilson has pointed out that in the absence of aliasing, halving the sampling interval and doubling the sample noise power must leave the final result unaltered. As a result, in the over-

sampled case, $0 < WT < 0.5$, the normalized deviations must be functions of only $(WT)/(S/N)$; in particular, the $S/N = 100$ and $S/N = 10$ curves of Figs. 8 and 9 for $0 < WT < 0.5$ must scale in the same way as described above for Figs. 4 and 5. This is most readily seen from present results by observing that for $0 < WT < 0.5$ all terms $\mathscr{A}(f \pm 1/T)$ in (27) through (30) disappear, and the noise and sampling interval appear only as the product NT. Thus the deviations remain unchanged as long as NT is fixed, i.e., if the number of samples and the signal-to-noise ratio are multiplied by the same factor.

Finally, we have an extremely simple result for the suboptimum filter for interpolation in the oversampled case, for both uniform and Gaussian illumination. Here $H(f)$ is given by (46). There is neither aliasing nor linear distortion, and substituting (46) into the third relation of (18) yields

$$\langle d_o^2(t) \rangle = S \cdot \frac{2WT}{S/N}. \tag{79}$$

The linear relation (80) yields the curves of Figs. 12 and 14 for $0 < WT < 0.5$. Again the normalized deviation depends only on $(WT)/(S/N)$.

APPENDIX D

Optimum Filters Minimize Time-Dependent Mean-Square Deviations

The optimum linear estimator for $x_o(t)$ of Fig. 2 (i.e., "interpolation") may be written as[8]

$$y(t) = \sum_k a_k(t)[x_o(kT) + n(kT)], \tag{80}$$

where $x_o(kT)$ and $n(kT)$ are the signal and noise samples of (8); the coefficients a_k, necessarily functions of time, are selected to minimize the mean-square deviation $d_o^2(t)$, where

$$d_o(t) \equiv y(t) - x_o(t). \tag{81}$$

The $a_k(t)$ satisfy[8]

$$\langle \{x_o(t) - \sum_k a_k(t)[x_o(kT) + n(kT)]\} \cdot \{x_o(iT) + n(iT)\} \rangle = 0. \tag{82}$$

Equation (82) yields

$$\phi_{x_o}(t - iT) - \sum_k a_k(t)\phi_{x_o}((k - i)T) + N \cdot a_i(t) = 0, \tag{83}$$

where N is the power of the (independent) noise samples (Fig. 2) and $\phi_{x_o}(\tau)$ is the covariance of $x_o(t)$, i.e., the Fourier transform of $P_{x_o}(f)$ of (1).

The index i and the summation index k in eqs. (82) and (83) range

over the set of samples used to estimate $x_o(t)$. While this set may be finite, the present work assumes an infinite number of samples are used. Then it is immediately obvious by the stationarity of $x_o(t)$ that

$$a_k(t) = a_0(t - kT) \equiv a(t - kT), \tag{84}$$

where we drop the subscript 0 as unnecessary. Substituting (84) into (80), the optimum estimator for $x_o(t)$ is

$$y(t) = \sum_{k=-\infty}^{\infty} [x_o(kT) + n(kT)]a(t - kT), \tag{85}$$

where $a(t)$ is given by

$$\phi_{x_o}(t) = \sum_{k=-\infty}^{\infty} \phi_{x_o}(kT)a(t - kT) + N \cdot a(t). \tag{86}$$

If we Fourier transform (86), use the Poisson sum formula, and solve for the transform of $a(t)$,

$$A(f) = \frac{P_{x_o}(f)}{\frac{1}{T}\sum_{k=-\infty}^{\infty} P_{x_o}\left(f - \frac{k}{T}\right) + N}. \tag{87}$$

Then, if we substitute (3) into (87), comparing (8) with (80), we identify $a(t)$ with $T \cdot h(t)$, and hence replace $A(f)$ by T times $H_o(f)$ of (27), to yield

$$H_o(f) = \frac{|\mathscr{X}(f)|^2}{\sum_{k=-\infty}^{\infty} \left|\mathscr{X}\left(f - \frac{k}{T}\right)\right|^2 + \frac{NT}{X}}. \tag{88}$$

Finally, imposing the constraint (17) and recalling that $\mathscr{X}(f)$ is strictly bandlimited to $|f| < W$ [Fig. 2 or (3) and (14)], (88) becomes identical to (27).

We recall that in the undersampled case ($0.5 < WT < 1$) the optimum interpolation filter $H_o(f)$ of (27) minimized the time-average mean-square deviation $\overline{\langle d_o^2(t)\rangle}$ of (6). The present appendix shows that $H_o(f)$ also minimizes the time-dependent mean-square deviation $\langle d_o^2(t)\rangle$ for all t.

A similar discussion may be given for restoration; the optimum filter $H_W(t)$ of (29), which minimizes $\overline{\langle d_W^2(t)\rangle}$, also minimizes $\langle d_W^2(t)\rangle$ for all t.

AUTHOR

Harrison E. Rowe, B.S., M.S., Sc.D. (Electrical Engineering), The Massachusetts Institute of Technology, 1948, 1950, 1952; U.S. Navy, 1945–1946, AT&T Bell Laboratories, 1952–1984; Stevens Institute of Technology, 1984—.

Mr. Rowe was a Member of Technical Staff in the Radio Research Laboratory prior to his retirement in 1984. Presently he is Anson Wood Burchard Professor of Electrical Engineering at Stevens. His publications include numerous papers and one textbook, spanning a variety of fields including parametric amplifiers, noise and communication theory, propagation in random media, and related problems in waveguide, radio, and optical communication systems. He is the joint author of five patents. Fellow, IEEE; corecipient, 1977 David Sarnoff Award and 1972 Microwave Prize; member, Commission C of URSI, Sigma Xi, Tau Beta Pi, and Eta Kappa Nu.